Int. J. Electrochem. Sci., 6 **(2011)** 3776 - 3788

International Journal of
ELECTROCHEMICAL
SCIENCE
www.electrochemsci.org

Membraneless Enzymatic Biofuel Cells Based on Multi-walled Carbon Nanotubes

Ying Li[1], *Shen-Ming Chen*[1,*], *Ramiah Sarawathi*[2]

[1] Department of Chemical Engineering and Biotechnology, National Taipei University of Technology, No.1, Section 3, Chung-Hsiao East Road , Taipei 106, Taiwan (ROC).
[2] Department of Materials Science,Madurai Kamaraj University, Madurai - 625 021, INDIA.
[*]E-mail: smchen78@ms15.hinet.net

Received: 15 July 2011 / *Accepted:* 5 August 2011 / *Published:* 1 September 2011

Multi-walled carbon nanotubes (MWCNTs) with glucose oxidase (GOx) are directly fabricated on glassy carbon electrode (GCE) and indium tin oxide electrode (ITO) by simple process. The MWCNTs/GOx modified ITO electrode surface has been studied in detail using scanning electron microscopy (SEM) and atomic force microscopy (AFM). This MWCNTs/GOx film modified GCE effectively exhibits the electro oxidation signals for the detection of glucose. MWCNTs provided large surface area for GOx base on modified electrode. The cyclic voltammetry (CVs) has been used for the measurement of electroanalytical properties of analytes by means of modified electrodes. The power densities of glucose biofuel cell based on the MWCNTs/GOx electrode was 65 $\mu W/cm^2$ at 0.58 V, respectively. The biofuel cell showed highly stable output in long term performance. Efforts are underway to improve the interface transfer to achieve higher potential and current output.

Keywords: Multi-walled carbon nanotubes (MWCNTs); Glucose oxidase (GOx); Glucose; Biofuel cell ; Membraneless, Electrochemical Reactions, Bioelectrochemistry.

1. INTRODUCTION

Global energy demands continue to increase every year. While petroleum products currently supply much of this demand, the increasing difficulty of sustained supply and the associated problems of pollution and global warming are acting as a major impetus for research into alternative renewable energy technologies [1]. Fuel cells are devices that convert chemical energy into electrical energy. Biofuel cells offer a possible solution to this problem, with the fuel needed for conventional cells usually being either hydrogen, methanol and glucose [2-3]. Biofuel cells have traditionally been classified as either microbial-based and enzymatic fuel cells according to whether the enzymes were located inside of microorganisms or outside of living cells [4]. The main benefits of enzyme-based

biofuel cells are the capability to produce biofuel cells orders of magnitude smaller than equivalently powered microbial cells and allowing operation to take place closer to the redox potential of the enzyme itself. For an efficient operation of an enzyme-based biofuel cell a number of conditions must be satisfied. The enzyme should have high catalytic activity, stability, and be inexpensive [5]. Enzyme-based fuel cells have remained a popular focus for research due to the high turnover rates associated with enzymes that lead to a high biocatalysis rate [6]. Glucose biofuel cells generate electricity through oxidation of glucose on the anode and reduction of oxygen on the cathode [7-11]. Glucose oxidase (GOx) may be the best enzyme for the biofuel cells [12-13]. GOx is stable, highly catalytically active, inexpensive, and glucose as a fuel is wide spread in the biological environment [14]. It comprises one flavin adenine dinucleotide ($FAD/FADH_2$) cofactor per monomer [15-16]. The $FAD/FADH_2$ is so deeply buried in the electrically insulating glycoprotein, ~15 Å below the protein surface, that it is not directly electrooxidized or electroreduced at an electrode surface [17-18]. In aqueous solution at pH 7.0, the redox potential for the active site of the enzyme $FAD/FADH_2$ is sufficiently negative for anode operation [19]. A major challenge is the $FAD/FADH_2$ redox center of GOx is located deeply in the apoenzyme [20-21].

Advances in nanoscience and nanotechnology have created a new direction for design and development of next generation electronic micro- and nanoscale materials and devices for industrial, pharmaceutical, clinical, environmental, space exploration, and defense applications [22-30]. Suitable electrode materials and immobilization methods of enzymes onto the electrode surface are important for obtaining their direct electrochemical reaction and keeping their bioactivities [31-32]. Carbon nanotube (CNT) is an attractive catalyst support because of its unique properties such as small size, large surface area, high electrical conductivity, and high chemical and thermal stability. For these reasons, conducting nanowires for fast electron transfer between the active site of an enzyme and the electrode surface of conventional carbon supports in fuel cell electrodes [33-55]. Recent studies in the field of multi-walled carbon nanotubes (MWNTs) modified electrodes demonstrated new perspectives for the nanodevice constructions. The MWNTs have a fast electrontransfer rate for different redox reactions and better electrical conductivity compared to single-walled carbon nanotubes. The unique properties of MWNTs as an electrode material include nanometer scale and well-graphitized structure, which can be used to construct three-dimensional nanoelectrode ensembles [56-58].

In this report, we have exploited unique properties of multi-walled carbon nanotubes for the fabrication of a glucose oxidase (GOx) electrode as an anode for biofuel cells based on electrode surface. We designed novel configuration biofuel cells for highly power density. The proposed method is simple and would be applicable to enhance the power output of miniaturized biofuel cell.

2. EXPERIMENTAL

2.1. Materials

Multi-walled carbon nanotubes (Aldrich) was used as received, Cetrimonium bromide (CTAB), Hydroquinone (HQ), Glucose oxidase (GOx) (EC1.1.3.4) were purchased from Sigma–Aldrich (St.

Louis, U.S.A.). All other chemicals used were of analytical grade and used without further purification 0.1 M pH 7.0 phosphate buffer solutions (PBS). Aqueous solutions were prepared using doubly distilled deionized water and then deaerated by purging with high purity nitrogen gas for about 20 min before performing electrochemical experiments. Also, a continuous flow of nitrogen over the aqueous solution was maintained during measurements.

2.2. Apparatus

Cyclic voltammetry (CVs) was performed in an analytical system model CHI-1205A potentiostat. A conventional three-electrode cell assembly consisting of an Ag/AgCl reference electrode and a Pt wire counter electrode were used for the electrochemical measurements. The working electrode (anode) was glassy carbon electrode (GCE; area 0.07 cm^2), cathode of electrode was platinum electrode (Pt; area 0.007 cm^2). In these experiments, all the potentials have been reported versus the Ag/AgCl reference electrode. The morphological characterizations of the films were examined by means of SEM (Hitachi S-3000H) and atomic force microscopy (AFM) (Being Nano-Instruments CSPM5000). The power output measurements system by KEITHLEY 2400. All the solutions were purged with high purity nitrogen gas for about 20 min before performing electrochemical experiments. Also, a continuous flow of nitrogen over the aqueous solution was maintained during measurements. All the experiments were carried out at room temperature (≈ 25°C).

2.3. Preparation of MWCNTs/glucose oxidase (GOx) modified electrodes

There was an important challenge in the preparation of MWCNTs. Because of its hydrophobic nature, it was difficult to disperse it in any aqueous solution to get a homogeneous mixture. Briefly, the hydrophobic nature of the MWCNTs was converted in to hydrophilic nature by following the previous studies [59-60]. This was done by weighing 10 mg of MWCNTs and 200 mg of potassium hydroxide in to a ruby mortar and grained together for 4 hr at room temperature. Then the reaction mixture was dissolved in 10 ml of double distilled deionized water and it was precipitated many times in to methanol for the removal of potassium hydroxide. A stable suspension of MWCNTs was obtained by dispersing the MWCNTs in a solution of surfactant, such as cetyltrimethylammonium bromide (CTAB, a cationic surfactant). MWCNTs (dispersed in the solution of 0.1% CTAB) MWCNTs (dispersed in the solution of 0.1% CTAB) has promotion effects homogeneous dispersion. Thus obtained MWCNTs was ultrasonicated for 6 hr to get a uniform dispersion. This functionalization process of MWCNTs was done to get a hydrophilic nature for the homogeneous dispersion. This process not only converts MWCNTs to hydrophilic nature but this helps to breakdown larger bundles of MWCNTs in to smaller ones also.

Prior to modification, glassy carbon electrode was polished with 0.05 μm alumina on Buehler felt pads and then ultrasonically cleaned for about a minute in water. Finally, the electrode was washed thoroughly with double distilled water and dried at room temperature. The cleaned glassy carbon electrode was coated with 2μL of MWCNTs and the solvent was allowed to evaporate at room

temperature.

The glucose oxidase (GOx) was immobilized onto the MWCNTs modified electrode surface by adsorption attachment. 2μL GOx solution (5 mg/ml in pH 7.0 PBS) was pipetted onto the electrode and the surface was dried for approximately 1 h at room temperature. The resulted modified electrode was stored in a refrigerator at 4 ◦C for use. The film formed on the electrode surface can be expressed as the Scheme 1.

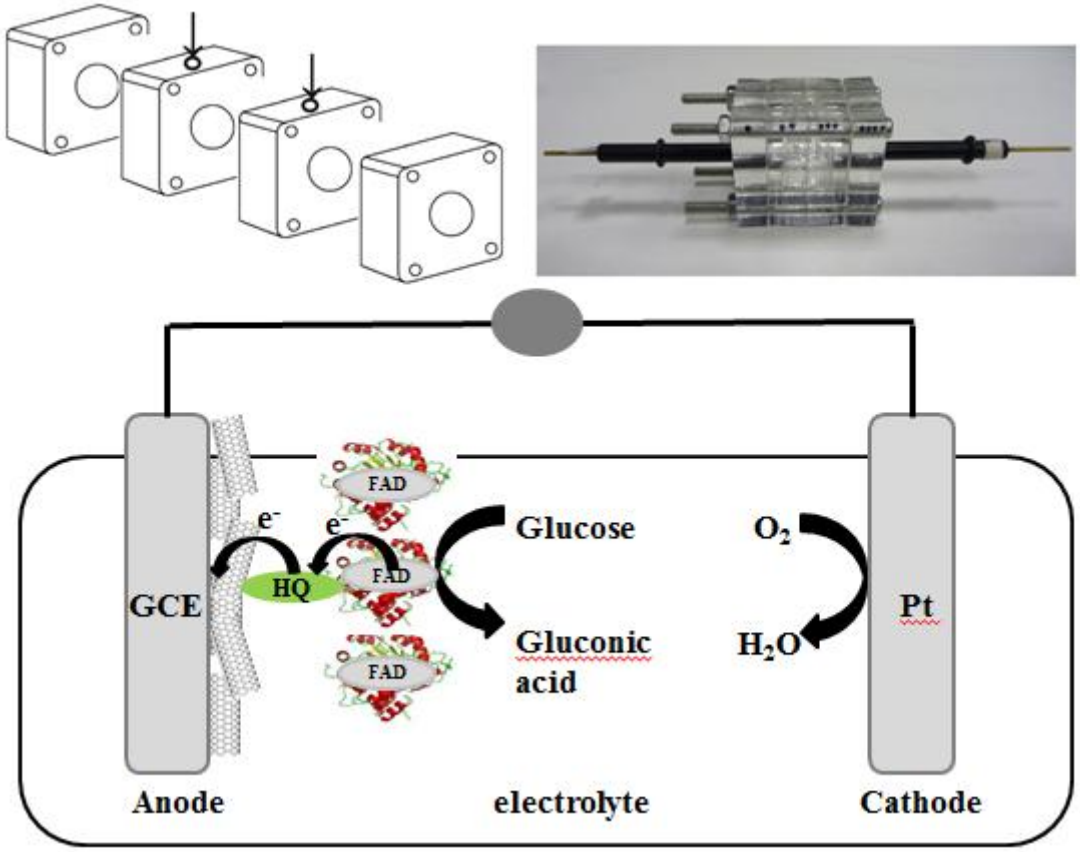

Scheme 1. A stack design for the configuration of biofuel cell with MWCNTs/GOx modified electrodes.

3. RESULTS AND DISCUSSIONS

3.1. Electrochemical characterizations of MWCNTs/GOx

In the following experiments, each newly prepared film on GCE has been washed carefully in deionized water to remove the loosely bound GOx on the modified electrode. It was then transferred to pH 7.0 PBS for the other electrochemical characterizations. These optimized pH solutions have been chosen to maintain the higher stability (pH = 7.0). Fig. 1 shows different types (a) only GOx, (b) MWCNTs and (c) MWCNTs/GOx. The corresponding cyclic voltammograms have been obtained at 100 mVs^{-1} scan rate in the potential range of -0.65 to -0.2 V. The redox peak current at formal

potential $E^{0,}$ = -0.39V represents the redox peak for GOx (curve c). Curve (a) of figure shows cyclic voltammetric response of GOx modified electrode. As can be seen, there is no obvious peak in the potential region studied. Curve (b) only MWCNTs modified electrode shows broad background current. From this figure, comparison of curve (a) and curve (c) , it is found that the presence of MWCNTs shows the currents increased, it is found that the presence of MWCNTs shows the catalytic effect on GOx redox peak currents.

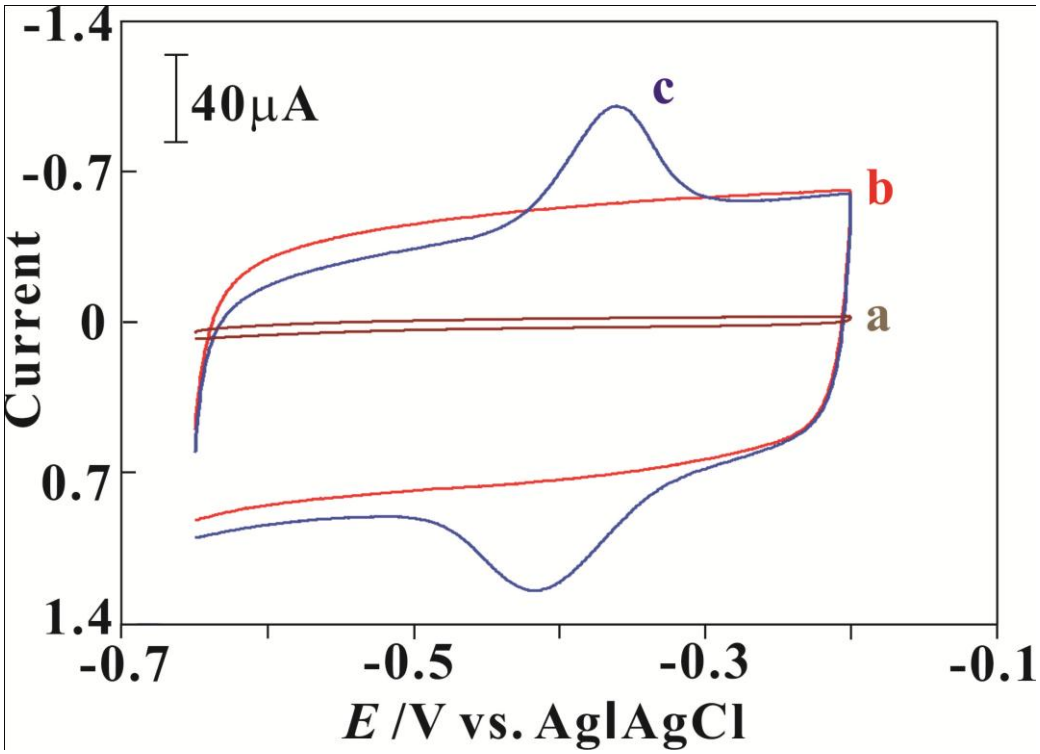

Figure 1. Cyclic voltammograms in 0.1 M PBS (pH = 7.0) for different electrodes: (a) only GOx; (b) MWCNTs; (c) MWCNTs/GOx, scan rate = 100mV s^{-1}.

Immobilization of enzymes to solid electrode surface is a key step for the design, fabrication and performance of the biosensor, since it is well known that some enzymes retain their activity when they are immobilized [61]. Inorder to confirm stability of modified electrode, the cyclic voltammetric of the MWCNTs/GOx electrode using PBS (pH = 7.0) at different scan rates (10 to 100 mV/s) . Fig. 2 shows that the anodic and cathodic peak currents of both the film redox couples which have increased linearly with the increase of scan rates. Calibration curve for data in figure 2 (a) shows I_{pa} & I_{pc} vs. scan rate, (b) I_{pa} & I_{pc} vs. scan rate$^{1/2}$. The ratio of I_{pa}/I_{pc} from the inset has demonstrated that the redox process has not been controlled by diffusion. However, the ΔE_p of each scan rate reveals that the peak separation of composite redox couple increases as the scan rate is increased.

Fig. 3 shows the cyclic voltammetric of MWCNTs/GOx on electrode obtained in PBS, then washed with deionized water and was transferred to various pH aqueous buffer solutions. This shows that the film is highly stable in the pH range between 1 to 13. The values of E_{pa} and E_{pc} depends on the

pH value of the buffer solution. The inset in Fig.3 shows the potential of MWCNTs/GOx plotted over a pH range from 1 to 13.

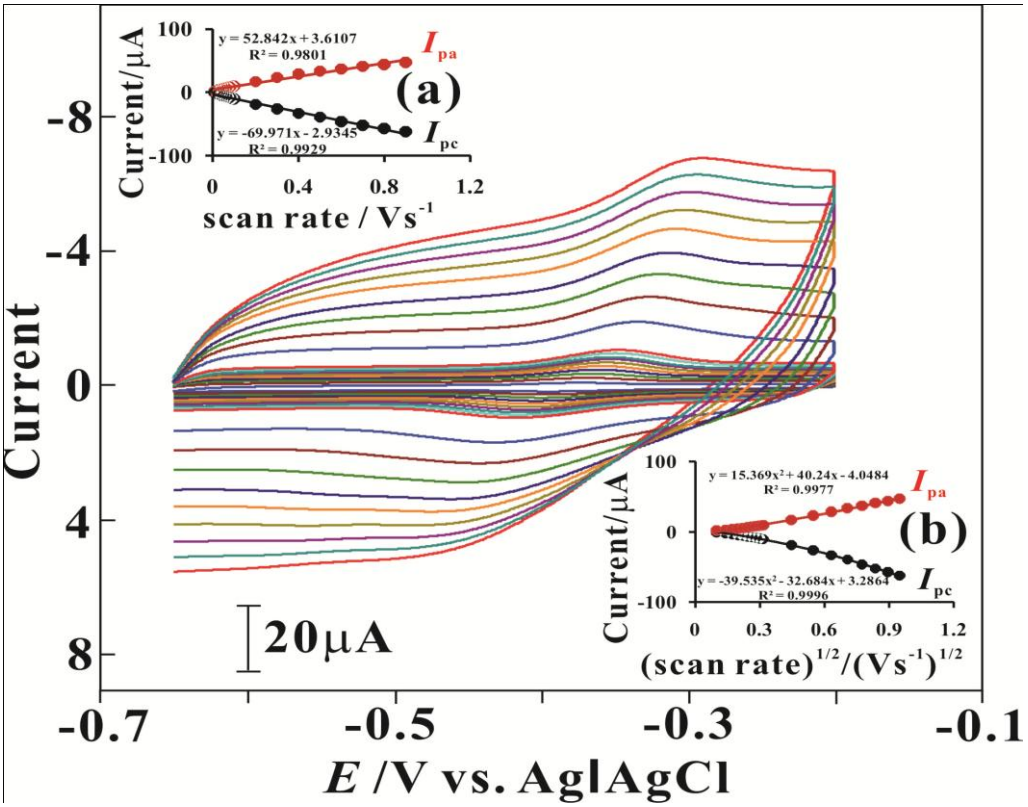

Figure 2. Cyclic voltammograms of 0.1 M PBS (pH = 7.0) at MWCNTs/GOx electrode at different scan rate from 10 mV s^{-1} to 1000 mV s^{-1}, respectively. Calibration curve for data shows I_{pa} & I_{pc} vs. (scan rate) and I_{pa} & I_{pc} vs. scan rate$^{1/2}$.

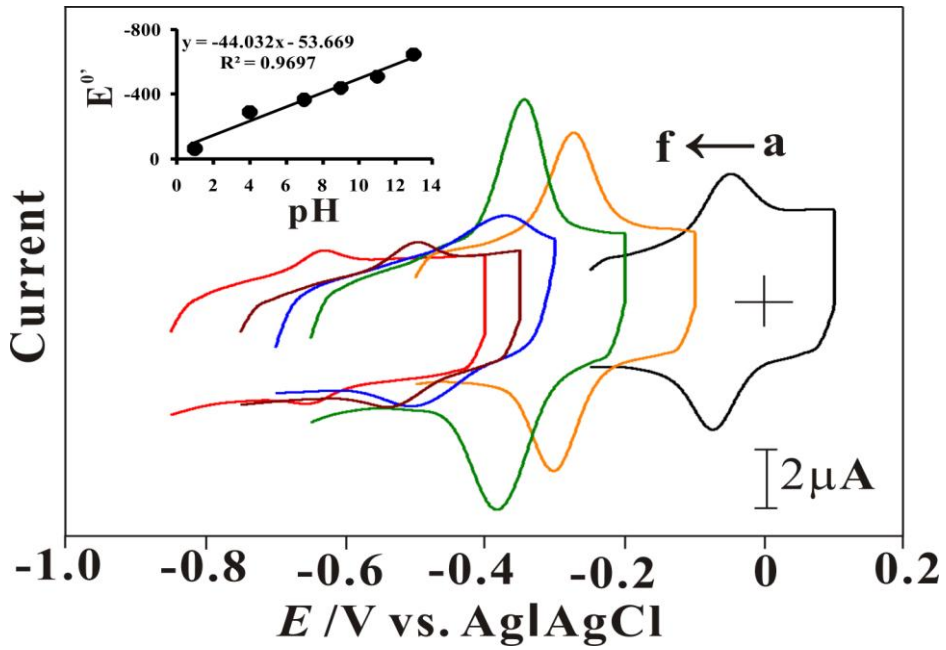

Figure 3. Cyclic voltammograms of the MWCNTs/GOx transferred to various (a) 1, (b) 4, (c) 7, (e) 9, (d) 11, (f) 13, pH solutions. The inset shows the formal $E^{0'}$ vs. pH.

3.2. Morphological characterization of MWCNTs/GOx film

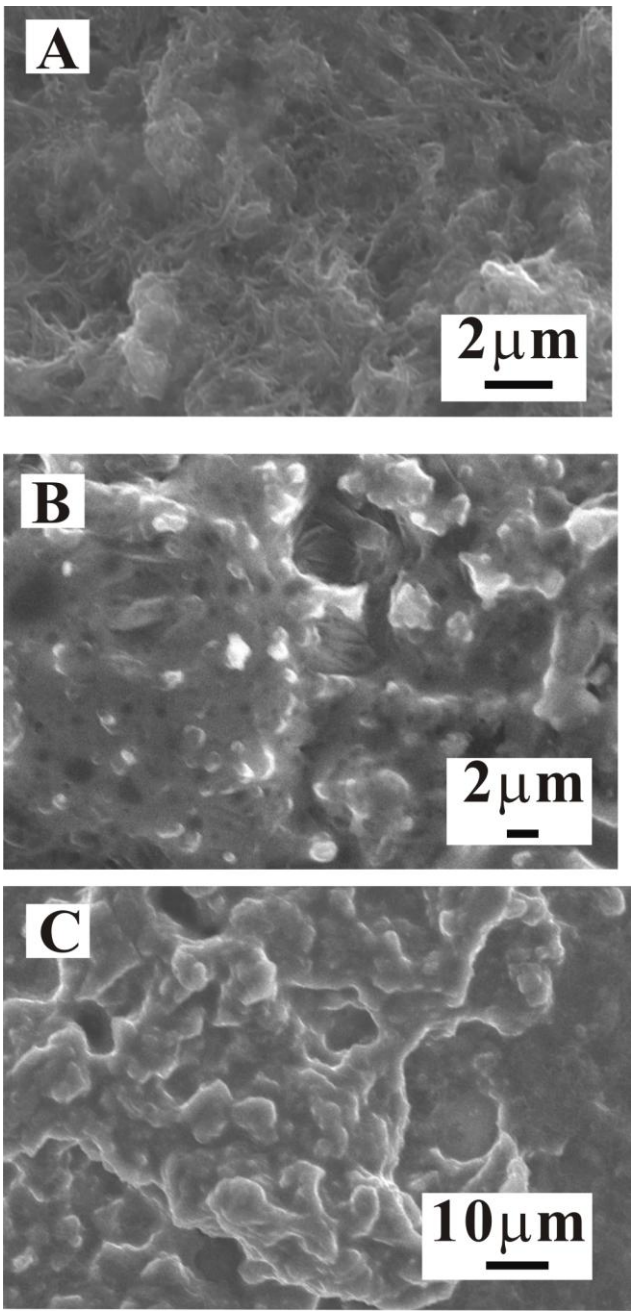

Figure 4. SEM images of (A) MWCNT; (B) only GOx; (D) MWCNTs/GOx on ITO electrode .

Over the last decade, biofuel cells have become a popular research area, and traditional analytical techniques have been tailored to study them. Electroanalytical techniques were the first to be used to characterize and understand bioelectrodes for biofuel cells, but recently, microscopic techniques have been adapted for use in this field. Using these techniques, researchers have developed a much more fundamental understanding of the properties of the bioelectrodes [60]. There are two commonly used electron microscopy techniques for imaging biofuel cell materials: scanning electron microscopy (SEM) and atomic force microscopy (AFM). Prior to modification, ITO surfaces were

cleaned and ultrasonicated in acetone–water mixture for 15 min and then dried. Further, three different films; MWCNTs, only GOx and MWCNTs/GOx have been prepared on the ITO electrode were characterized using SEM.

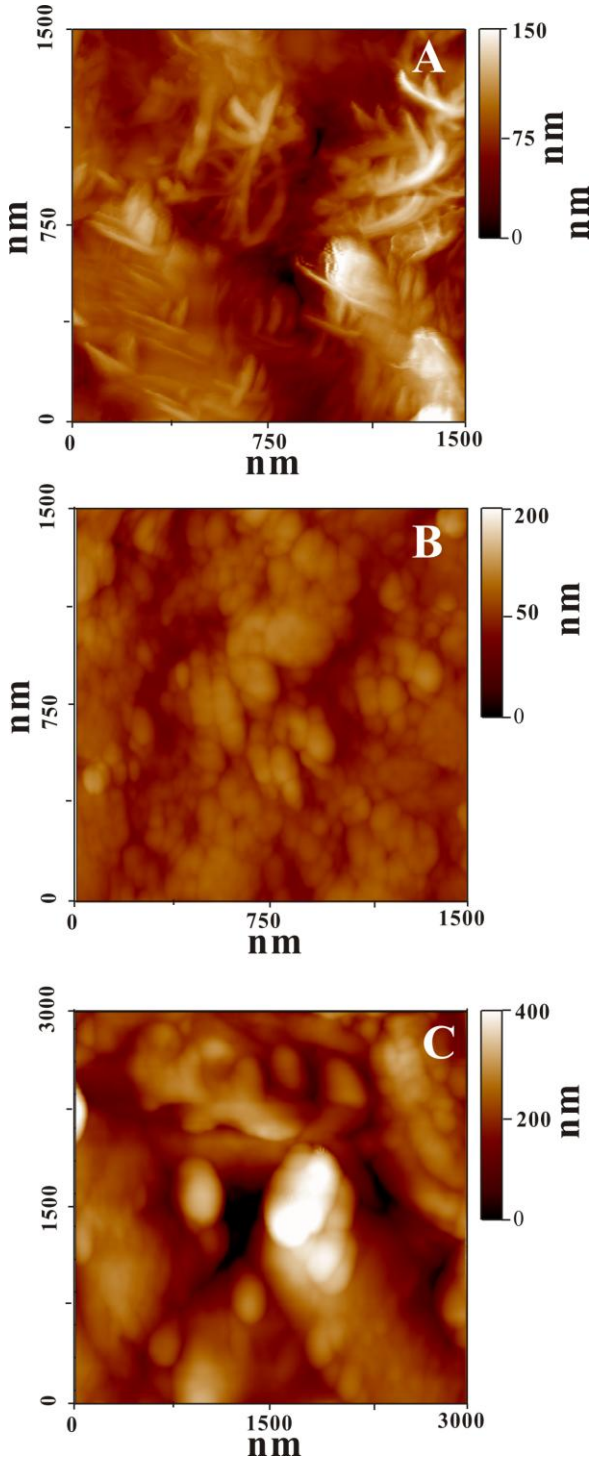

Figure 5. AFM images of (A) MWCNT; (B) only GOx; (D) MWCNTs/GOx on ITO electrode .

From Fig. 4, it is significant that there are morphological differences between both the films. It is a well known fact that the prolonged exposure to the electron beam will damage the GOx films, so

an utmost care was taken to measure these images. The top views of nano structures Fig. 4 (A) on the ITO electrode surface shows uniformly deposited homogeneously dispersed MWCNTs on this electrode. The MWCNTs/GOx film in Fig. 4 (C) reveals that the GOx had covered the entire MWCNTs. Comparison of (B) only GOx and (C) MWCNTs/GOx reveals, these results could be explained as the increase in deposition of GOx presence of MWCNTs. We can clearly see that the immersed MWCNTs/GOx have been gathered together. The same modified ITO electrodes have been used to measure the AFM topography images of Fig. 5 (A) MWCNTs, (B) only GOx, (C) MWCNTs/GOx electrode. In all these cases the observed morphological structure is similar to that of SEM.

3.3. Electroanalytical response of glucose at MWCNTs/GOx film

The MWCNTs/GOx film was synthesized on GCE at similar conditions as described in Materials and Methods.

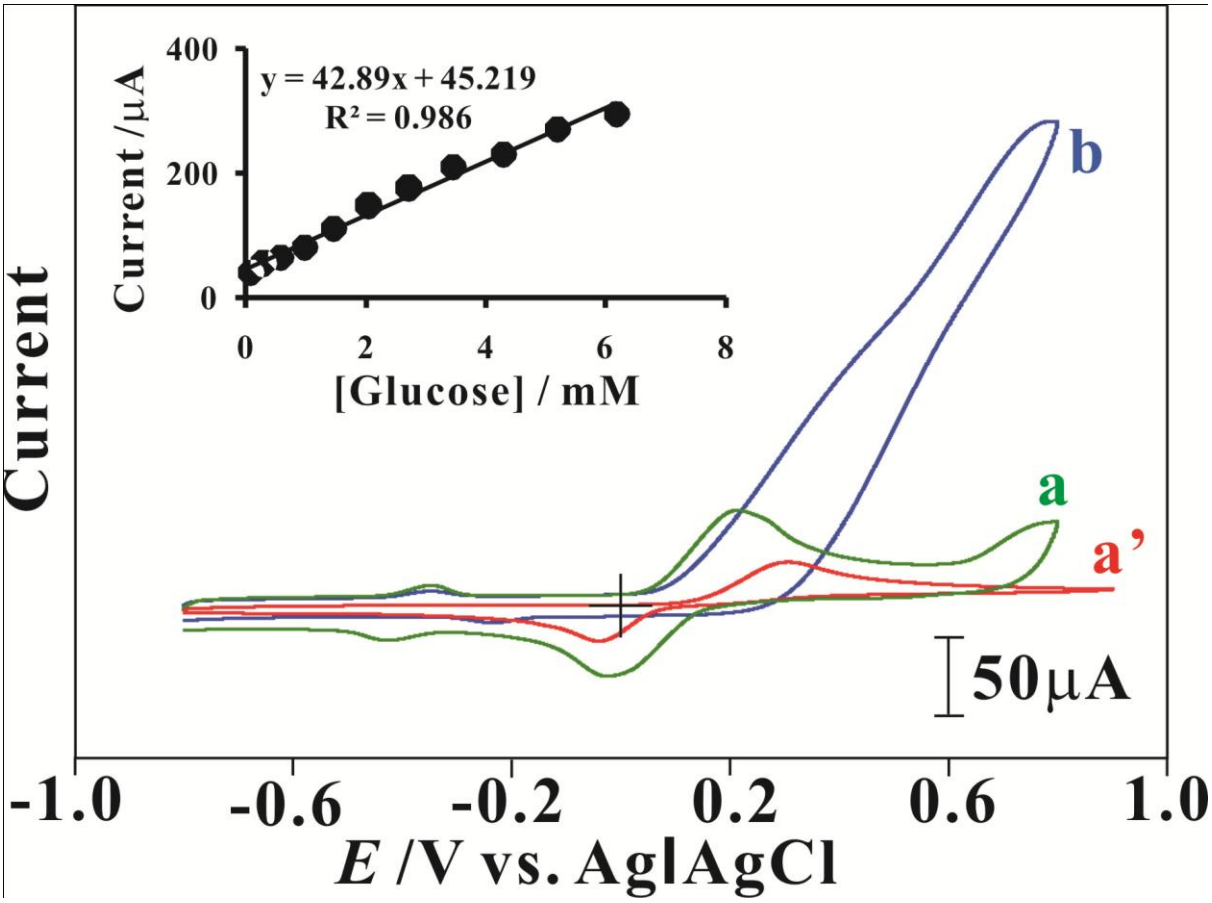

Figure 6. Cyclic voltammograms of different electrodes in pH=7.0 PBS containing 1 mM Hydroquinone (HQ) with 5 mM glucose, scan rate = 100 mV s^{-1}: (a') bare GCE and (b) MWCNTs/GOx; (a) MWCNTs/GOx in the absence of glucose. Inset shows a current vs. concentration plot of glucose at MWCNTs/GOx electrode.

Then the MWCNTs/GOx modified electrode was washed carefully in deionized water and transferred to pH 7.0 PBS for the electrocatalysis of glucose. All of the CVs were recorded at the constant time interval of 2 min with nitrogen purging before the start of each experiment. The enzymatic reaction in the use of GOx as a receptor can be described as follows:

$$\text{FAD} + \text{glucose} \xrightarrow{\text{GOx}} \text{FADH}_2 + \text{Gluconolactone} \quad \text{(Enzymatic)} \qquad (1)$$

$$\text{FADH}_2 \xrightarrow{\text{HQ}} \text{FAD} + 2\text{H}^+ + 2\text{e}^- \quad \text{(Electrochemical)} \qquad (2)$$

Fig. 6 shows the electrocatalytic oxidation of glucose. Curve (a') bare GCE and (b) MWCNTs/GOx; (a) MWCNTs/GOx (absence of glucose) in pH=7.0 PBS containing 1 mM hydroquinone (HQ) with 5 mM glucose, scan rate = 100 mV s^{-1} in the potential range of -0.5 to 0.5 V. Inset shows a current vs. concentration plot of glucose at MWCNTs/GOx electrode. Upon addition of glucose a new growth in the oxidation peak at 788 mV of respective analytes have appeared at the current values. An increase in concentration of glucose, simultaneously produced a linear increase in the oxidation peak currents of the glucose. Oxidation of glucose by the biocatalyst yields the reduced $FADH_2$ redox site. The hydroquinone (HQ) mediates oxidation of $FADH_2$ and further electron transfer to the electrode. As the quinone is exposed to the electrode surface, its rapid oxidation by the conductive support allows the cyclic electrochemically induced oxidation of glucose. The observations at bare electrode (curve a') clearly indicate that the fouling effect of the electrode surface with the oxidation obtaining the weak single peak for glucose. From all these above results it is clear that MWCNTs/GOx film is more efficient and exhibits enhanced functional properties compared to that of bare alone.

3.5. Biofuel cell performance of MWCNTs/GOx modified anode

As model for a membraneless biofuel cell working under physiological conditions, the MWNTs/GOx modified electrode was applied as anode together with a Pt electrode as cathode in a 5 mM solution of glucose in pH 7.0 PBS containing 1 mM hydroquinone (HQ). The application of the MWNTs/GOx modified electrode for the biofuel cell has been demonstrated during GOx electrode testing in galvanostatic regime (Fig. 7). Analysis has shown that the catalytic electrooxidation current of glucose appears at 0.58 V with a current density of 0.02 μA/cm^2 and reaches 59 μA/cm^2 at 0 V vs. Ag/AgCl. Current density was calculated versus geometric electrode area, giving 0.07 cm^2. The open circuit potential (OCV) (0.58V) of the glucose oxidase (GOx) modified electrode is close to the redox potential of the $FAD/FADH_2$ cofactor in the enzyme itself. Thus, MWCNTs/GOx electrodes based on membraneless electron transfer between the active site of the enzyme and MWCNTs offer promising solutions for generations of biofuel cells. As the current is produced, the cell voltage starts to decrease, the cell voltage drops faster and become 0 Vat 59 μA/cm^2 of the short circuit current (SCC). From the measured I–V curves, maximum power densities are calculated to be 65 μW/cm^2 .

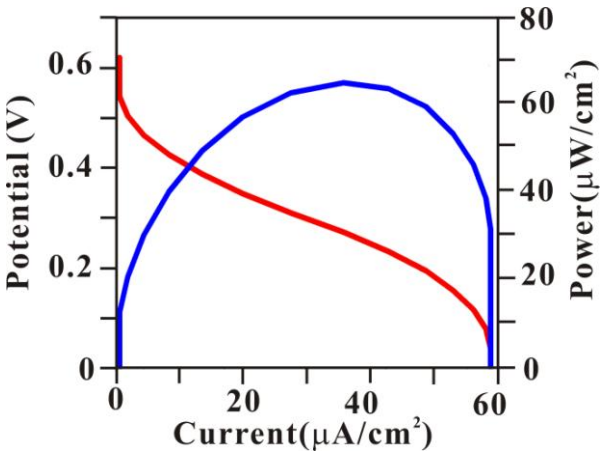

Figure 7. Polarization curve (red) and dependence of the power density on the operating voltage (blue) for a membrane-less biofuel cell consisting of MWCNTs/GOx modified electrode as anode in combination with a Pt electrode as cathode. As fuel a 5 mM solution of glucose in PBS (pH 7.0) containing 1 mM hydroquinone (HQ) was used.

4. CONCLUSIONS

We have demonstrated application of MWCNTs/GOx modified electrode for biofuel cell. The modified electrode showed stable response. High sensitivity and stability together with very easy preparation makes MWCNTs/GOx electrode as promising candidate for constructing simple electrochemical sensor for glucose. The SEM and AFM results have shown the difference between type films morphological data. Further, it has been found that the MWCNTs/GOx has an excellent functional property along with good electrocatalytic activity on glucose. The experimental methods of CVs with film biosensor integrated into the GCE which are presented in this paper, provide an opportunity for qualitative and quantitative characterization, even at physiologically relevant conditions. Thus, glucose biofuel cell anodes with increased coulombic efficiency far beyond the usual yield of two electrons per substrate molecule can be developed. Besides glucose, a variety of other substrates can be oxidized by these anodes. It is expected that this easy fabrication of enzyme electrodes will paves the way for the development of a new generation of biofuel cells and also will be useful for the development of bioreactors and biosensors.

ACKNOWLEDGEMENT
Financial support from the National Science Council of Taiwan and the Department of Science and Technology, India under Indo-Taiwan Science and Technology Program is gratefully acknowledged.

References

1. E. Kjeang, D. Sinton, D.A. Harrington, *J. Power Sources* 158 (2006) 1–12.
2. F.D. Bruijn, *Green Chem.* 7 (2005) 132-150.
3. V.S. Bagotzky, N.V. Osetrova, A.M. Skundin, *Russ. J. Electrochem.* 39 (2003) 919-934.

4. S.C. Barton, J. Gallaway, P. Atanasov, *Chem. Rev.* 104 (2004) 4867-4886.
5. S.D. Minteer, B.Y. Liaw, M.J. Cooney, *Curr. Opin. Biotechno.* 18 (2007) 228–234.
6. F. Davis, S.P.J. Higson, *Biosens. Bioelectron.* 22 (2007) 1224–1235.
7. E. Katz, O. Lioubashevski, I. Willner, *J. Am. Chem. Soc.* 127 (2005) 3979–3988.
8. E. Katz, I. Willner, *J. Am. Chem. Soc.* 125 (2003) 6803–6813.
9. N. Mano, F. Mao, A. Heller, *J. Am. Chem. Soc.* 124 (2002) 12962–12963.
10. R.F. Service, *Science* 296 (2002) 1223–11223.
11. I.Willner, *Science* 298 (2002) 2407–2408.
12. A.Heller, A., *Chem. Phys.* 6 (2004) 209–216.
13. A.Heller, B. Feldman, *Chem. Rev.* 108 (2008)2482–2505.
14. R. Wilson, A.P.F. Turner, *Biosens. Bioelectron.* 7 (1992) 165-185.
15. A.Vaze, N. Hussain, C. Tang, D. Leech, J. Rusling, *Electrochem. Commun.* 11 (2009) 2004–2007.
16. K.C. Lin, S.M. Chen, *Biosens. Bioelectron.* 21 (2006) 1737-1745.
17. A.Prévoteau, O. Courjean, N. Mano, *Electrochem. Commun.* 12 (2010) 213–215.
18. Q. Chi, J. Zhang, S. Dong, E. Wang, *Electrochim. Acta* 39 (1994) 2431-2438.
19. A.G. Elie, C. Lei, R.H. Baughman, *Nanotechnology* 13 (2002) 559-564.
20. C. Cai, J. Chen, *Anal. Biochem.* 332 (2004) 75-83.
21. W. Liang, Y. Zhuobin, *Sensors* 3 (2003) 544-554.
22. S.E. McNeil, *J. Leukoc. Biol.* 78 (2005) 585-594.
23. K.K. Jain, *Clin. Chim. Acta* 358 (2005) 37-54.
24. G.S. Sayler, M.L. Simpson, C.D. Cox, *Curr. Opin. Microbiol.* 7 (2004) 267-273.
25. Y. Choi, G.Wang, M.H. Nayfeh, S.T. Yau, *Biosens. Bioelectron.* 24 (2009) 3103–3107.
26. C. Zou, Y. Fu, Q. Xie, S. Yao, *Biosens. Bioelectron.* 25 (2010) 1277–1282.
27. J. Kim, S.I. Kim, K.H. Yoo, *Biosens. Bioelectron.* 25 (2009) 350–355.
28. X. Lu, J. Zhou, W. Lu, Q. Liu, J. Li, *Biosens. Bioelectron.* 23 (2008) 1236–1243.
29. M.R. Majidi, K.A. Zeynali , B. Hafezi, *Int. J. Electrochem. Sci.*, 6 **(**2011**)** 162–170.
30. A.R. Taheri, A. Mohadesi, D. Afzali, H.K. Maleh, H. Mahmoudi, Moghaddam, H. Zamani, Z.R. zad, *Int. J. Electrochem. Sci.*, 6 **(**2011**)** 171 –180.
31. C. Cai, J. Chen, *Anal. Biochem.* 332 (2004) 75–83.
32. G. Merle, A. Habrioux, K. Servat, M. Rolland, C. Innocent, K.B. Kokoh, S. Tingry, *Electrochimica Acta* 54 (2009) 2998–3003.
33. Y. Li, Y. Umasankar, S.M. Chen, *Talanta* 79 (2009) 486–492.
34. Y. Li, Y. Umasankar, S.M. Chen, *Anal. Biochem.* 388 (2009) 288–295.
35. Y. Umasankar, Y. Li, S.M. Chen, *J. Electrochem. Soc.* 157 (2010) K187-K193.
36. W. Chen, J. Zhao, J.Y. Lee, Z. Liu, *Mater. Chem. Phys.* 91 (2005) 124–129.
37. W. Li, C. Liang, J. Qiu, W. Zhou, H. Han, Z. Wei, G. Sun, Q. Xin, *Carbon* 40 (2002) 791–794.
38. Z. Liu, X. Lin, J.Y. Lee, W. Zhang, M. Han, L.M. Gan, *Langmuir* 18 (2002) 4054–4060.
39. X. Sun, R. Li, D. Villers, J.P. Dodelet, S. Desilets, *Chem. Phys. Lett.* 379 (2003) 99–104.
40. C. Wang, M. Waje, X. Wang, J.M. Tang, R.C. Haddon, Y. Yan, *Nano Lett.* 4 (2004) 345–348.
41. Y.L. Yao, Y. Ding, L.S. Ye, X.H. Xia, *Carbon* 44 (2006) 62–66.
42. J.S. Ye, H.F. Cui, Y. Wen, W.D. Zhang, G.Q. Xu, F.S. Sheu, *Microchim. Acta* 152 (2006) 267–275.
43. Y. Zhao, L. Fan, H. Zhong, Y. Li, S. Yang, *Adv. Funct. Mater.* 17 (2007) 1537–1541.
44. J. Wang, M. Musameh, *Anal. Chem.* 75 (2003) 2075–2079.
45. R.R. Schlittler, J.W. Seo, J.K. Gimzewski, C. Durkan, M.S.M. Saifullah, M.E. Welland, *Science* 292 (2001) 1136–1139.
46. J. Tans, A.R.M. Verschueren, C. Dekker, *Nature* 393 (1998) 49–52.
47. M. Musameh, J. Wang, A. Merkoci, Y. Lin, *Electrochem. Commun.* 4 (2002) 743–746.
48. J. Wang, M. Li, Z. Shi, N. Li, Z. Gu, *Anal. Chem.* 74 (2002) 1993–1997.

49. X. Yin, D. Chattopadhyay, I. Galeska, F. Papadimitrakopoulos, J.F. Rusling, *Electrochem. Commun.* 5 (2003) 408–411.
50. J.J. Gooding, R. Wibowo, J. Liu, W. Yang, D. Losic, S. Orbons, F.J. Mearns, J.G. Shapter, D.B. Hibbert, *J. Am. Chem. Soc.* 125 (2003) 9006–9007.
51. J. Wang, R.P. Deo, P. Poulin, M. Mangey, *J. Am. Chem. Soc.* 125 (2003) 14706–14707.
52. J. Chen, J.C. Bao, C.X. Cai, T.H. Lu, *Chin. Chem. Lett.* 14 (2003)1171–1174.
53. C.X. Cai, *J. Chen, Anal. Biochem.* 325 (2004) 285–292.
54. J. Chen, C.X. Cai, *Chin. J. Chem.* 22 (2004) 167–171.
55. J. Li, A. Cassell, L. Delzeit, J. Han, M. Meyyappan, *J. Phys. Chem. B* 106 (2002) 9299-9273.
56. S.G. Wang, Q. Zhang, R. Wang, S.F. Yoon, *Biochem. Biophys. Res. Commun.* 311 (2003) 572-576.
57. C. Wang, M. Waje, X. Wang, J.M. Tang, R.C. Haddon, Y. Yan, *Nano Lett.* 4 (2004) 345-348.
58. Y. Yan, M. Zhang, K. Gong, L. Su, Z. Guo, L. Mao, *Chem. Mater.* 17 (2005) 3457–3463.
59. U. Yogeswaran, S.M. Chen, *J. Electrochem. Soc.* 154 (2007) E178–E186.
60. A.Salimi, R. Hallaj, S. Soltanianb, *Electroanalysis* 21 (2009) 2693-2700.
61. M.J. Moehlenbrock, R.L. Arechederra, K.H. Sjö holm, S.D. Minteer, *Anal. Chem.* 81 (2009) 9538–9545.